Hindawi
Advances in Civil Engineering
Volume 2023, Article ID 4286038, 9 pages
https://doi.org/10.1155/2023/4286038

*Research Article*

# An Improved Approach of Classical Upper Bound Theory for Stability Analysis of Layered Slopes

**ZeRun Tian**,[1] **YanHong Zhang**,[1] **XiTong Wei**,[2] **Fei Li**,[1] **and YaFeng Guo**[1]

[1]*College of Water Resources and Hydropower Engineering, Gansu Agricultural University, Lanzhou 730070, China*
[2]*PLA(Troop77115), Chendu 611230, China*

Correspondence should be addressed to YanHong Zhang; zhyh9606@163.com

Received 25 May 2023; Revised 27 July 2023; Accepted 2 August 2023; Published 25 September 2023

Academic Editor: Paolo Castaldo



The equations for the critical height of layered slope were derived by a related researcher, but they lack details and do not agree with the method of limit equilibrium. So this topic was reinvestigated. Considering the possible global or local failure modes of the layered slope, the equations for the critical height of the above modes are derived based on the upper limit theorem by using rotational failure mechanisms or rotational and translational failure mechanisms. Based on the above theory, the stability coefficients of layered slope are investigated. The results show that the presented upper bound approach has better performance than other methods mentioned in the literature and is consistent with the limit equilibrium method. In combination with the strength reduction method, the global and local stability of the layered slope are analyzed using the several examples. The high-calculation accuracy of presented method and the specific measures to improve the smoothness of the sliding surface are reviewed. From the perspective of the combination of sliding surfaces, the dimensionless parameter vector of the layered slope is introduced. The possible limitations of the upper bound limit approach with log spirals are pointed out and the conditions which must be fulfilled in order to achieve a higher computational accuracy are mentioned.

## 1. Introduction

Slope stability analysis is an important component of the geotechnical engineering. The economic consequences of landslides are significant, as they can endanger human life and property [1]. After more than half a century, several methods for the analysis of slope stability have been proposed and applied: the best known are the limit equilibrium method (LEM), which is based on a fundamentally empirical background, and the finite element method (FEM). The former was first proposed by Fellenius [2], and other methods, such as those of Bishop [3], Morgenstern and Price [4], Spencer [5], and Sarma [6], are constantly applied and developed. However, there are no theoretical reasons that sufficiently explain the success of the extensive applications, and the analysis results are not the upper and lower bounds of the true solution. The FEM, without assumptions on the failure mode, the numerical approach through elastoplastic, can deal with a wide range of practical problems. With the shear strength reduction (SSR) technique, elastoplastic FEM provides a powerful tool for the geotechnical stability analysis. Nevertheless, there are inconsistencies in the slip criterion and constitutive relations, as well as convergence problems. As another attractive alternative for slope stability estimation, limit analysis is widely applied and studied due to its distinct advantages. With this method, lower and upper boundary solutions can be determined, which can define the range of the true solution.

The earliest study of the upper bound method focuses on the homogeneous slopes. For the first time, the upper bound theorem of limit analysis was applied to the geotechnical problems and an explicit expression for the critical height of the homogeneous slope was derived by Chen et al. [7]. In his book "Limit analysis and soil plasticity," he described the principles of the upper and lower bound theorems of plasticity when applied to soil mechanics [8]. Later, Karal [9, 10] improved the upper bound method and derived the expression for the slope safety factor. Michalowski [11] presented another upper bound method with translational failure mechanism for the slope stability analysis, in which the block

was divided vertically for landslides, and later (2002) presented stability diagrams for uniform slopes [12]. Kumar [13] developed a detailed step-by-step procedure for calculating the factor of safety (FOS) of a slope. Later (2004), he used the concept of energy balance to calculate stability numbers of soil slopes with nonassociated coaxial and noncoaxial flow rules [14].

Some attention has previously been given to the studies of inhomogeneous slopes, which are much more common in real situations. Chen [8] used the kinematic approach to evaluate the stability of inhomogeneous and anisotropic slopes, assuming a logarithmic spiral failure surface but a uniform friction angle. Donald and Chen [15] proposed an upper bound method in which the sliding block was divided into several inclined slices. Chen et al. [16] and Chen [17] extended this solution domain to three dimensions and active earth pressure. Later, Nian et al. [18] used reinforcing piles to evaluate the slope stability in inhomogeneous and anisotropic soils and combined the kinematic approach with the SSR technique. Recently, several studies have extended the kinematic analysis technique to three-dimensional (3D) conditions [19]. Kumar and Samui [20] and Sun et al. [21] have each presented their own analysis methods with upper bounds for heterogeneous slopes. The latter considered the variation of shear strength parameters with soil depth by the spatial discretization technique, but there were still some problems that could not be ignored. Wang et al. [22] creatively transformed the composite slope into a single homogeneous slope and presented a limit analysis method suitable for the stability of 3D composite slopes. Chwała [23] proposed an upper boundary analysis method using a dashed line to simulate the failure mechanism of the dissipation zone of slopes with spatially variable properties.

Based on the theory of plastic limit analysis, Professor Sloan proposed a more widely applicable finite element limit analysis (FELA) method without assuming a failure mechanism by combining the generalized variational principle and the mixed FEM using either linear programing or nonlinear programing methods. Subsequently, some researchers [24–27] have gradually proposed more rigorous theoretical formulas for the upper and lower bounds. This method is currently applicable to rigid plastic or elasticplastic soils, and to various yield criteria and uncorrelated yield rules, and has been adopted by the geotechnical engineering software *OPTUM*. However, the computational efficiency of this method may decrease as the number of unit grids increases. Therefore, it is important to propose a more efficient and simpler stability analysis methods for stratified slopes, which are commonly used in practice.

Despite the extensive research that has been conducted since the critical slope height equation proposed by Chen [8], this classical method of strict upper bound method of slope has not been fully developed in the field of heterogeneous slopes because of the numerical difficulties [15]. But not enough attention has been paid to the critical slope height, which is important for excavation, design, and backcalculation of the slopes. Therefore, although the above researches on the upper limit analysis method are effective and applicable, there are still the following deficiencies.

(1) Explicit expressions for the critical height of the slope were not given. And the mechanism of partial rotation and partial instantaneous failure under the local stable failure mode was not fully considered.
(2) In particular, the results of the method proposed by Kumar and Samui [20] and Sun et al. [21] are not compatible with those of the method of limit equilibrium in some examples.
(3) The limits of the approach of the upper bound with logarithmic spirals could not be shown.
(4) In the finite element limit analysis method, the computational efficiency depends on the number of finite elements.

In this study, continuing the research of Chen and the above researchers, the expressions for the critical slope height at different failure modes were derived. The causes of the excessive calculation error of the upper bound method are discussed qualitatively, and the conditions that must be satisfied for higher calculation accuracy of the upper bound method are indicated.

## 2. Upper Bound Theorem

The upper bound theorem states that if the rate of external work (gravity) is equal to the rate of energy dissipation in any kinematically admissible velocity field, the solution is the upper bound of the true solution. In the kinematic approach, the main task in deriving the critical slope height is usually to assume a collapse mechanism and to determine the rate of external work and internal energy dissipation.

*2.1. Collapse Mechanism.* Two types of sliding surfaces, the combination logarithmic spirals (CLS) and the CLS with line (CLSL), are adopted, respectively, for the failure modes of global and local stability of layered slope. In both, all logarithmic spirals have a common pivot point, but in the latter, the straight line represents the instantaneous translational motion of the slope's rigid soil mass, as shown in Figures 1 and 2.

As shown in Figure 1, a layered slope with $n$ soil layers has a slope toe $E_n$, slope vertex $E_1$ or $e_1$, slope height $H$, slope angle $\beta$ and $\beta'$. The boundary line between two adjacent soil layers (i.e., soil $i$ and soil $i+1$) has points $E_i$ and $e_i$ with a horizontal slope angle $\alpha_i$ and intersection point $A_i$ with the sliding surface of the slope. And the main material parameters of slope of the $i$ layer are $\gamma_i$, $c_i$, $\varphi_i$. Each layer of soil $i$ has a thickness $m_i$ $H$ and a slip line which can be defined by a logarithmic spiral as follows:

$$r = r_i \exp[(\theta - \theta_i)\tan\varphi_i], \tag{1}$$

where $r$ and $r_i$ are the radii of rotation. The former lies between an angle of $\theta_i$ and $\theta_{i+1}$, the latter corresponds to an angle of $\theta_i$. The $v_i$ in Figures 1 and 2 represent the velocity field of the sliding rigid blocks in the slope, with an angle of $\varphi_i$ between the velocity field and the tangent to the sliding surface. To facilitate the derivation of the formula, the exponential parts of $r_i$ are denoted as $G_i$, and expressed as follows:

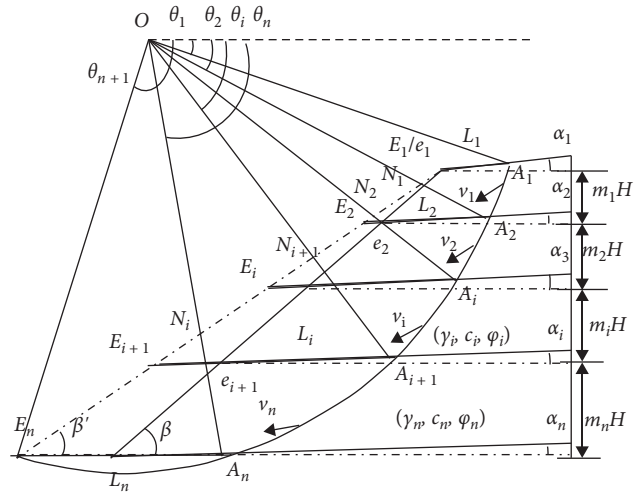


FIGURE 1: Collapse mechanisms of the layered slope (global stability).

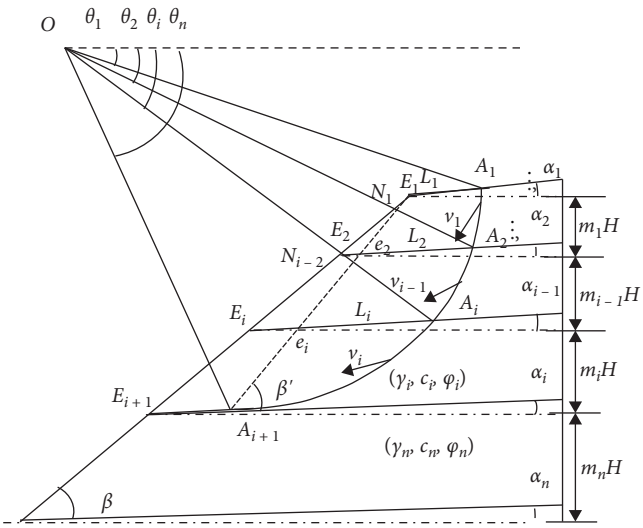


FIGURE 2: Collapse mechanisms of the layered slope (local stability).

$$r_i = r_{i-1}\exp[(\theta_i - \theta_{i-1})\tan\varphi_i] = r_1 G_i, \tag{2}$$

where $G_i$ expressed as follows:

$$G_i = \prod_{i=2}^{i}\exp[(\theta_i - \theta_{i-1})\tan\varphi_i],\ (i = 1, G_1 = 1). \tag{3}$$

For the slope with local failure, the soil mass above the logarithmic spirals is assumed to rotate about a common pivot point in the limit state of equilibrium, while the soil above the straight slip line undergoes an instantaneous translational motion. The above motions must satisfy the condition of velocity continuity, which is expressed as follows:

$$\theta_i = \frac{\pi}{2} + \varphi_i - \alpha_i. \tag{4}$$

Note that the height ratio coefficient $m_i$ cannot be applied directly, but must be converted to the virtual height ratio coefficient $m_i'$ in the following form

$$m_i' = \sum_{i=1} m_i\left[1 + \frac{\sin\beta'\sin\alpha_{i+1}}{\sin(\beta' - \alpha_{i+1})}(\cot\beta' - \cot\beta)\right] - \sum_{i=2}^{i-1} m_{i-1}'. \tag{5}$$

Although the slip line in Figure 1 is different from that in Figure 2, it is obvious that Figure 2 is a special case of Figure 1. So, it takes the same form.

Similar to Chen's [8] derivation, the geometric relationships of the layered slope are given as follows:

$$H/r_1 = \sin\beta'/\sin(\beta' - \alpha_1)\{G_{n+1}\sin(\theta_{n+1} + \alpha_1) - \sin(\theta_1 + \alpha_1)\}, \tag{6}$$

$$L_i/r_1 = G_i\sin(\beta' - \alpha_i)\{G_i\sin(\theta_{n+1} + \alpha_1) - G_{n+1}\sin(\theta_1 + \alpha_1)\}. \tag{7}$$

The stability analysis process based on the critical slope height formula is essentially an optimization process. For the collapse mechanism of CLS, the optimized parameters are $\theta_1$, $\theta_{n+1}$ and $\beta'$, and for CLSL, the optimized parameters are $\theta_1$ and $\beta'$, but there are more intermediate nonindependent variables, such as $\theta_2$, $\theta_3$, …, $\theta_n$ in Figures 1 and 2. These variables are determined by the following equation.

$$\begin{cases} m_2'/m_1' = (M_3 - M_2)/(M_2 - M_1) \\ \vdots \\ m_i'/m_{i-1}' = (M_{i+1} - M_i)/(M_i - M_{i-1}) \\ \vdots \\ m_n'/m_{n-1}' = (M_{n+1} - M_n)/(M_n - M_{n-1}) \\ M_{n+2} = M_{n+1} \end{cases}, \tag{8}$$

where $M_i$ is expressed in the form

$$M_i = G_i\left[\sin\left(\theta_i + \frac{L_i}{r_i}\sin a_i\right)\right]. \tag{9}$$

*2.2. External Power Rate.* Researchers believe that it is difficult to integrate the external work of the stratified slope, but in reality there is no such difficulty for the stratified slope, and the calculation of the external force shows regularity. For the $i$-layered slope, in Figure 1, the external power rate can be expressed as follows:

$$W_i = W_{OA_iA_{i+1}} + W_{N_iA_{i+1}E_{i+1}} - W_{OE_iA_i} - W_{OE_iN_i} - W_{E_ie_ie_{i+1}E_{i+1}}. \tag{10}$$

It can be simplified as follows:

$$W_i = \gamma_i \Omega \left[ f_{OA_iA_{i+1}} + f_{N_iA_{i+1}E_{i+1}} - f_{OE_iA_i} - f_{OE_iN_i} - f_{E_ie_ie_{i+1}E_{i+1}} \right], \tag{11}$$

where $\gamma_i$ is unit weight, $\Omega$ is angular velocity, $f_{OA_iA_{i+1}}$ and $f_{N_iA_{i+1}E_{i+1}}$, $f_{OE_iA_i}$, $f_{OE_iN_i}$, $f_{E_ie_ie_{i+1}E_{i+1}}$ are, respectively, expressed as follows:

$$f_{OA_iA_{i+1}} = \frac{G_i^3}{3(1+9[\tan\varphi_i]^2)} \left\{ (3\tan\varphi_i \cos\theta_{i+1} + \sin\theta_{i+1}) \frac{G_{i+1}^3}{G_i^3} - (3\tan\varphi_i \cos\theta_{i+1} + \sin\theta_i) \right\}, \tag{12}$$

$$f_{N_iA_{i+1}E_{i+1}} = \frac{\sin(\beta' - \alpha_{i+1})\sin(\theta_{i+1} + a_{i+1})}{6\sin(\beta' + \theta_{i+1})} \left(\frac{L_{i+1}}{r_1}\right)^2 \left\{ 3G_{i+1}\cos\theta_{i+1} - \frac{L_{i+1}}{r_1} \left( \frac{\cos\theta_{i+1}\sin(\beta' - a_{i+1})}{\sin(\beta' + \theta_{i+1})} + \cos\alpha_{i+1} \right) \right\}, \tag{13}$$

$$f_{OE_iA_i} = \frac{1}{6}\left(\frac{L_i}{r_i}\right)^2 \left\{ 2\cos\theta_i - \frac{L_i}{r_i}\cos\alpha_i \right\} \sin(\theta_i + \alpha_i) G_i^3, \tag{14}$$

$$f_{OE_iN_i} = \frac{1}{6} G_{n+1} \sin(\theta_{n+1} + \beta') \left\{ \frac{m_i'}{\sin\beta'} \frac{H}{r_1} - \frac{L_{i+1}}{r_{i+1}} \frac{\sin(\theta_i + a_i)}{\sin(\beta' + \theta_i)} \right\}, \tag{15}$$

$$f_{E_ie_ie_{i+1}E_{i+1}} = f(i+1) - f(i), \tag{16}$$

in which, $f(i)$ is written as follows:

$$f(i) = \frac{1}{6} \sum_{i=2}^{i} m_{i-1}' \sum_{i=2}^{i} m_{i-1} \left(\frac{H}{r_1}\right)^2 (\cot\beta' - \cot\beta) \left\{ 3G_{n+1}\cos\theta_{n+1} + \frac{H}{r_1} \left[ 3\cot\beta' - \sum_{i=2}^{i} \left( m_{i-1}' \cot\beta' + m_{i-1}\cot\beta \right) \right] \right\}, \ (i = 1, f(i) = 0). \tag{17}$$

*2.3. Internal Energy Dissipation Rate.* Considering the upper bound theorem, the slip surface can be regarded as the surface of the velocity discontinuity. However, if one follows the associated flow laws and the Mohr–Coulomb criterion, this inevitably leads to the consumption of frictional and dilational energy balancing out. By integration, the rate of internal energy dissipation occurring in the velocity discontinuity surface can be written as follows:

$$\overline{E} = \sum c_i \left( G_{i+1}^2 - G_i^2 \right) / 2\tan\varphi_i. \tag{18}$$

For local failure, both the log spirals and the linear section have internal energy dissipation, so the internal energy dissipation rate can be expressed as follows:

$$\overline{E} = \sum c_i \left( G_{i+1}^2 - G_i^2 \right) / 2\tan\varphi_i + c_i (\cot\beta' - \cot\beta)\cos\varphi_i \frac{H}{r_1}. \tag{19}$$

*2.4. Critical Heights of Layered Soil Slope.* When the rate of external work equals to $\overline{E}$, the soil mass of the slope reaches the limit equilibrium state. Therefore, the critical height of an $n$-layered slope can be expressed as follows:

$$H_{cr} = \frac{\sum c_i \left( G_{i+1}^2 - G_i^2 \right) / 2\tan\varphi_i}{\sum f_i \gamma_i} \frac{H}{r_1}, \tag{20}$$

in which $H/r_1$ is shown in Equation (6).

It can be seen that for the layered slope with different material parameters, there is no form of the stability coefficient corresponding to that of the homogeneous slope. For the local failure mode, the similar equation for the critical height can be formulated as follows:

$$H_{cr} = \frac{\sum c_i \left( G_{i+1}^2 - G_i^2 \right) / 2\tan\varphi_i + c_i (\cot\beta' - \cot\beta)\cos\varphi_i H / r_1}{\sum f_i \gamma_i} \frac{H}{r_1}. \tag{21}$$

By using the above formula in conjunction with SSR, the slope stability analysis problem can be transformed into an optimization problem. When the critical height $H_{cr}$ is exactly equal to the actual height of the slope, the reduction coefficient is the slope stability FOS.

## 3. Evaluation of Analytical Methods

In order to test and analyze the effectiveness and limitations of the proposed approach and to provide a method for improving the smoothness of the sliding surface, three main examples are presented in this work.

Table 1: The stability coefficients $N_s$ of Chen [8] and Sun et al. [21] and this work.

| $\varphi$(°) | Source | $\beta$° | | | | | | |
|---|---|---|---|---|---|---|---|---|
| | | 15° | 25° | 35° | 45° | 55° | 65° | 75° |
| 5° | Chen [8] | 14.38 | 10.02 | 8.41 | 7.35 | 6.53 | 5.81 | 5.14 |
| | Sun et al. [21] | 14.30 | 9.99 | 8.38 | 7.33 | 6.53 | 5.79 | 5.12 |
| | Present | 14.37 | 10.12 | 8.41 | 7.35 | 6.53 | 5.81 | 5.14 |
| 10° | Chen [8] | 45.49 | 16.64 | 11.61 | 9.31 | 7.84 | 6.73 | 5.80 |
| | Sun et al. [21] | 44.99 | 16.57 | 11.61 | 9.29 | 7.83 | 6.72 | 5.80 |
| | Present | 45.49 | 16.64 | 11.61 | 9.31 | 7.84 | 6.73 | 5.80 |
| 15° | Chen [8] | — | 32.11 | 16.83 | 12.05 | 9.54 | 7.85 | 6.57 |
| | Sun et al. [21] | — | 31.96 | 16.78 | 12.04 | 9.53 | 7.84 | 6.56 |
| | Present | | 32.11 | 16.83 | 12.05 | 9.54 | 7.85 | 6.57 |
| 20° | Chen [8] | — | 94.63 | 26.66 | 16.16 | 11.80 | 9.25 | 7.48 |
| | Sun et al. [21] | — | 93.74 | 26.58 | 16.14 | 11.78 | 9.24 | 7.49 |
| | Present | | 94.63 | 26.66 | 16.16 | 11.80 | 9.25 | 7.48 |

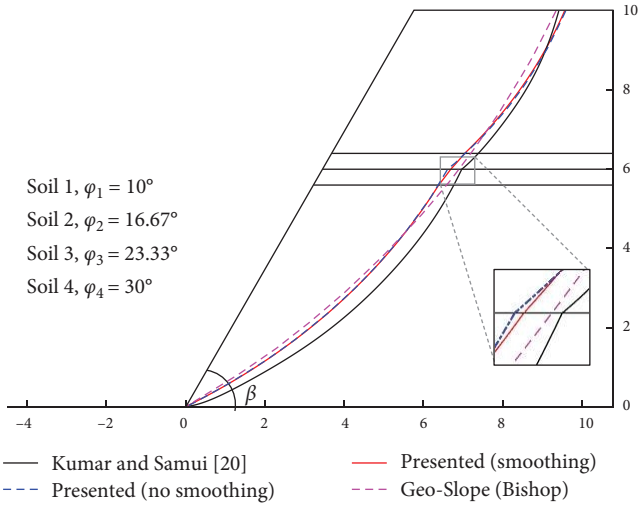


Figure 3: Results of slope stability analysis with $\beta$ of 60° and $\varphi_2$ of 30°.

*3.1. Verification and Discussion (Global Failure Mode).* According to Equation (20), a multilayered slope naturally degenerates into a homogeneous slope when soil parameters are the same. Chen [8] has given the stability coefficients $N_s$ ($N_s = \gamma H/c$) of homogeneous slopes in the range of friction angle from 5° to 20°, which cover most cases of practical engineering applications. As shown in Table 1, the stability coefficients in this work are almost identical to those of Chen [8] and Sun et al. [21] while Sun's results are smaller, which may lead to a larger FOS in the slope stability analysis.

To investigate the performance of the presented method for the layered slope, the first example of Kumar and Samui [20], whose critical equation for the layered slope is worth reevaluating, was used with $m_1$ of 0.4, $m_2$ of 0.6, $\gamma$ of 17.8 kN/m$^3$, $c$ of 14.3 kN/m$^2$, $\varphi_1$ of 10°, $\varphi_2$ of 20°, and the geological profile in Figure 3. Comparing the results of this work with those of Kumar and Samui [20] and Sun et al. [21], as shown in Table 2, one can see that the stability coefficients of the three are close to each other. However, when $m$ is equal to 0.4, and $\beta$ is equal to 45°, 70° and 80°, the stability coefficients in this work are obviously different from the others, and the comparison results show that the results of Kumar and Samui [20] and Sun et al. [21] have a relative error of 19% and 12%, respectively, compared with the Morgenstern–Price method (by Geo-Slope software), but not more than 3% in this work. The main reason for this phenomenon is that the computational accuracy of the method of Sun et al. [21] can be affected by the number of skew strips and the rationality of the allowed velocity field. However, Kumar et al. did not provide a detailed equation for the critical height of the slope, so the reason is unclear. Thus, the proposed method can determine the slope stability coefficients in greater agreement with the method of limit equilibrium, which shows the advantage of the presented upper bound approach.

To further investigate the performance of this method in analyzing slope stability, the case of Kumar [13] with $\varphi_2$ of 30° is reexamined. As shown in Table 3 and Figure 3, the slope stability of the presented upper bound method is very close to that of Kumar and Samui [20], Deng et al. [28], and Zhao et al. [29]. However, Kumar's FOS is smaller and the sliding surface of the slope is deeper.

Because of the material differences between the topsoil and subsoil, there is an obvious discontinuity at the intersection of the logarithmic spirals, as shown in Figure 3. Although this discontinuity does not affect the analysis results, it does not correspond to reality, and the direction of the shear stress is not clear because the stress curve is. This unresolved contradiction is caused by the difference of the shear expansion angle between two adjacent layers, which can be improved by the linear layer transition technique. That is, the slope of two layers with different shear strength parameters is layered near the boundary $N$ times ($N = 2$), and the shear strength parameters of each layer are linearly transitioned between the lower layer and the upper layer. Although the problem cannot be completely solved, the sliding surface at the intersection tends to become smooth as the number of layers increases.

Without losing generality, the second example of Deng et al. [28] is studied with three layers, based on the LEM, with the slope parameters in Table 4. The results show that the

Table 2: Comparison of $N_s$ between researchers and the presented for layered slopes with $\varphi_2$ of 20° (Example 1).

| $m$ | Source | $\beta$ | | | | | | | |
|---|---|---|---|---|---|---|---|---|---|
| | | 45° | 50° | 55° | 60° | 65° | 70° | 75° | 80° |
| 0.2 | Kumar and Samui [20] | 15.69 | 13.60 | 11.86 | 10.30 | 8.95 | 7.89 | 7.06 | 6.32 |
| | Sun et al. [21] | —— | 13.51 | 11.72 | 10.30 | 9.22 | 8.29 | 7.46 | 6.77 |
| | Present | 15.61 | 13.51 | 11.73 | 10.33 | 9.23 | 8.30 | 7.49 | 6.78 |
| 0.4 | Kumar and Samui [20] | 13.86 | 12.10 | 10.78 | 9.47 | 8.5 | 7.55 | 6.06 | 5.56 |
| | Sun et al. [21] | —— | 12.84 | 11.21 | 9.94 | 8.91 | 7.29 | 6.61 | 5.81 |
| | Present | 15.06 | 12.85 | 11.22 | 9.96 | 8.92 | 8.36 | 7.30 | 6.62 |
| | Geo-Slope (Morgenstern–Price) | 15.31 | —— | —— | —— | —— | 8.30 | 7.51 | 6.80 |
| 0.6 | Kumar and Samui [20] | 13.26 | 11.78 | 10.48 | 9.22 | 8.25 | 7.31 | 6.6 | 5.95 |
| | Sun et al. [21] | —— | 11.70 | 10.63 | 9.24 | 8.35 | 7.59 | 6.91 | 6.31 |
| | Present | 13.53 | 11.72 | 10.34 | 9.26 | 8.36 | 7.59 | 6.92 | 6.31 |

Table 3: Comparison of the stability results with $\varphi_2$ of 30°.

| Reference | Analytical methods | Slope FOS |
|---|---|---|
| Kumar and Samui [20] | Upper bound approach | 1 |
| Deng et al. [28] | Morgenstern–Price | 1.093 |
| Zhao et al. [29] | Bishop | 1.080 |
| Presented | No smoothing | 1.061 |
| | Smoothing | 1.062 |
| Geo-Slope (Software) | Morgenstern-Price/Bishop | 1.086/1.084 |

Table 4: Slope parameters in layered slope (Example 2).

| Slope number | Shape parameters | | Soil parameters | | |
|---|---|---|---|---|---|
| | $m$ | $\delta_i$ (°) | Unit weight $\gamma$ (kN/m$^3$) | Cohesion $c$ (kN/m$^2$) | Friction angle $\varphi$ (°) |
| Soil 1 | 1/3 | 0 | 17.8 | 30 | 20 |
| Soil 2 | 1/3 | 10 | —— | 15 | 10 |
| Soil 2 | 1/3 | −10 | —— | 30 | 20 |

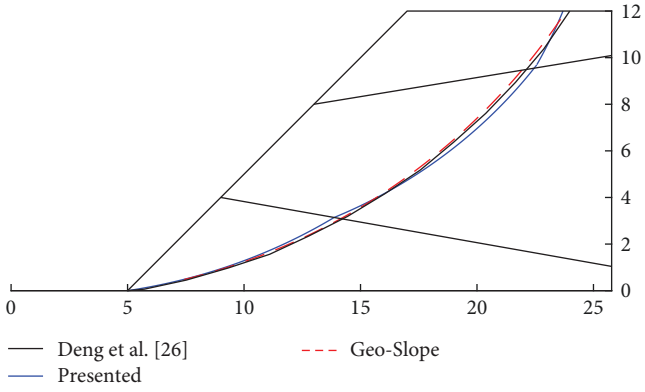


Figure 4: Results of slope stability analysis (Example 2).

accuracy of the upper limit method is comparable to that of the LEM for stability analysis of slopes with more than two layers, and the slip surfaces of the three methods are very close, as shown in Figure 4 and Table 5.

Table 5: Comparison of the stability results from Example 2.

| Reference | Analytical methods | Slope FOS |
|---|---|---|
| Deng et al. [28] | Morgenstern–Price | 1.188 |
| Presented | Upper bound approach | 1.196 |
| Geo-Slope | Bishop | 1.202 |

It is worth noting that the upper bound method based on the CLS does not always achieve high accuracy. It is considered that the relative error between the upper bound method and the LEM depends mainly on the selected combination type of the slope slip surface, which is given by the dimensionless parameter $\lambda = c/(\gamma H \tan \varphi)$ of Jiang and Yamagami [30]. This parameter is valid only for homogeneous slopes, but it can be extended to layered slope in the form

$$\vec{\lambda} = \left[\frac{c_1}{c_2}, \frac{c_1}{c_3} \cdots \frac{c_1}{c_n}, \lambda_1, \lambda_2, \cdots, \lambda_n\right]. \quad (22)$$

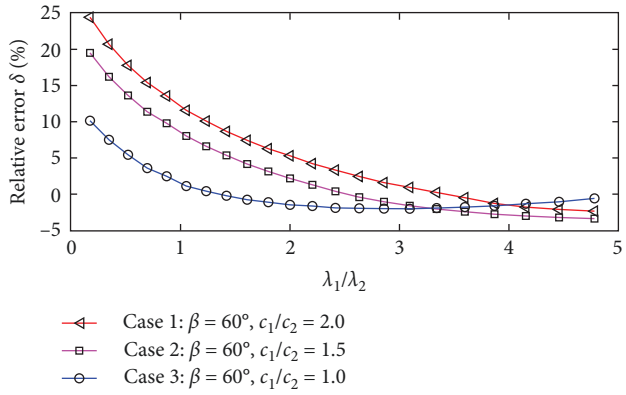


FIGURE 5: Relative error analysis of Kumar's example ($\beta$ of 60°).

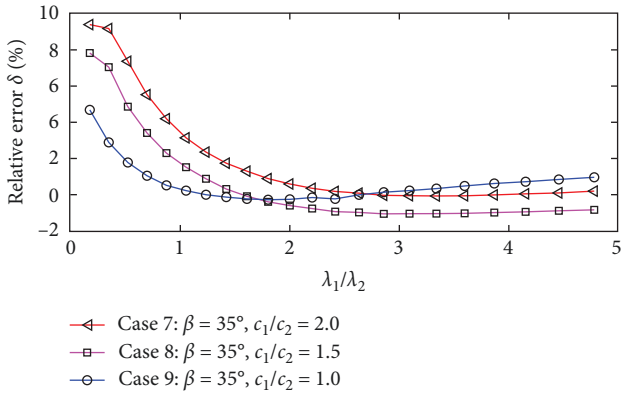


FIGURE 7: Relative error analysis of Kumar's example ($\beta$ of 35°).

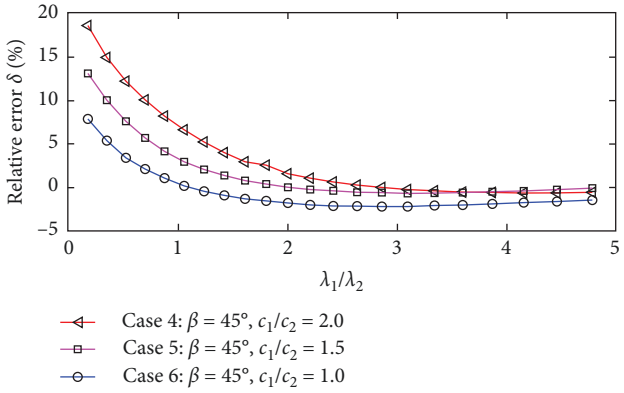


FIGURE 6: Relative error analysis of Kumar's example ($\beta$ of 45°).

And the correspondence between dimensionless vector and sliding surface can be proved by similar approach of Jiang and Yamagami [30].

To evaluate the influence of the difference of the dimensionless parameter vector $\vec{\lambda}$, which reflects the combination mode of the slip plane, on the relative error $\delta$, Kumar's example was used several times for the slope stability analysis with $c_2$ of 14.38 kN/m$^2$ and $\lambda_1$ of 4, but with $\varphi_2$ of $[2^\circ, 4^\circ, \cdots, 44^\circ]$. Comparing the relative error of slope stability FOS between the upper bound method approach and Bishop's method provided by *Geo-Slope*, we can see that the upper bound method with CLS has limitations. When the slope is steeper and $\lambda_1/\lambda_2$ is smaller, the relative error $\delta$ between the two methods is up to 24%, which decreases as the slope slows down and increases as the cohesive force ratio increases, as shown in Figures 5–7. This phenomenon may be caused not only by the assumption of the slip plane, but also by the fact that the associated flow law overestimates the dilatancy angle of the soil, which causes the frictional energy consumption and dilatancy energy consumption to be opposite to each other. According to the research of Wang et al. [31], for homogeneous rectangular slopes, the unassociated flow laws can be used to obtain a larger slope stability coefficient or a smaller FOS. If the uncorrelated rule is used in the stability analysis, the boundary may be broken, which is not considered due to the relationship between the uncorrelated flow law and the normal stress on the sliding slope. Therefore, the upper bound approach using the CLS failure mechanism is only suitable for situations where the cohesion ratio is smaller and the dimensionless parameters are larger. Otherwise, a relative error of more than 5% may occur.

*3.2. Verification and Analysis (Local Failure Mode).* Equation (20) has been fully verified and evaluated by the above. However, if the shear strength of the upper layer is lower, local failure of the layered slope may occur. To verify Equation (21), the third example of a slope with four layers from Zolfaghari et al. [32] is used (water pressure and earthquake loads are not considered). The slope parameters are listed in Table 6, and the analysis results are shown in Tables 6 and 7 and Figure 8.

The method presented in this paper yields essentially the same slope FOS as those of Zolfaghari et al. [32] and Cheng et al. [33] using the methods of Morgenstern–Price and Spencer. The relative error is less than 2%, and the sliding surfaces of the slope are close to each other, which proves that the upper bound method using CLSL can analyze the local stability of the slope with high precision.

Table 6: Slope parameters in the layered slope (Example 3).

| (i) Slope number | Shape parameters | | Soil parameters | | |
|---|---|---|---|---|---|
| | $H_i$ (m) | $\delta_i$ (°) | Unitweight $\gamma$ (kN/m$^3$) | Cohesion $c$ (kN/m$^2$) | Friction angle $\varphi$ (°) |
| Soil 1 | 2 | 0 | 19 | 15 | 20 |
| Soil 2 | 3 | 0.6366 | —— | 17 | 21 |
| Soil 3 | 1 | 0 | —— | 5 | 10 |
| Soil 4 | 2.5 | 0 | —— | 35 | 28 |

Table 7: Comparison of the results of slope FOS (Example 3).

| Reference | Analytical method | Slope FOS |
|---|---|---|
| Zolfaghari et al. [32] | Morgenstern–Price | 1.48 |
| Cheng et al. [33] | Spencer | 1.4802 |
| Presented study | Upper bound approach | 1.452 |
| Geo-Slope | MorgensternPrice | 1.446 |

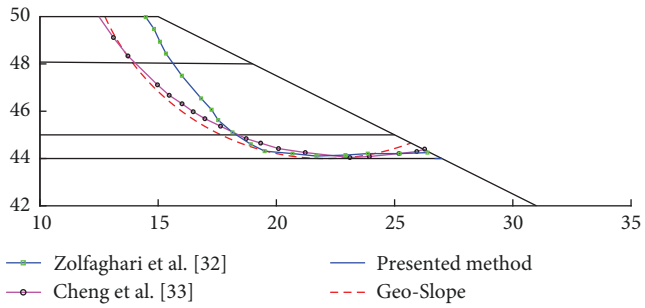


Figure 8: Analysis results of slope local stability (Example 3).

## 4. Conclusions

The equations for critical height of slopes are important for geotechnical engineering, but there is hardly any effective equation for critical height suitable for layered slope. In this paper, this issue is studied in detail and the following main conclusions are drawn.

(1) The derived equations for the critical height of layered slope have high precision and are in better agreement with the method of limit equilibrium, which confirms the advantages of these equations.

(2) The presented technique of layered slope linearization can effectively improve the problem of discontinuity of the sliding surface, but the safety factor of slope stability has not changed significantly.

(3) A dimensionless vector is presented that can reflect the relationship between the sliding surface and the shear strength parameters. On the basis of this vector, the limits of the upper bound method with CLS are shown and the slope of the application of the upper bound method with CLS is given.

## Data Availability

The authors confirm that the data supporting the findings of this study are available within the article.

## Conflicts of Interest

The authors declare that they have no conflicts of interest.

## Acknowledgments

This research was funded by the Key Research and Development Program of Gansu Province in China (20YF3FA036), the Innovation Fund Project of Higher Education in Gansu Province (2020A-048), and Gansu Agricultural University (Gaucwky-06). The authors thank the editors and reviewers for their valuable comments and suggestions.

## Supplementary Materials

*Name of the Code/Library*. Figure 3: slope stability analysis code 1 (Example 1, Figure 3); Figure 4: slope stability analysis code 2 (Example 2, Figure 4); Figure 8: slope stability analysis code 3 (Example 3, Figure 8). (*Supplementary Materials*)

## References

[1] R. L. Schuster, "Socioeconomic significance of landslides," in *Landslides: Investigation and Mitigation*, A. K. Turner and R. L. Schuster, Eds., pp. 12–35, National Academy Press, Washington, DC, 1996.

[2] W. Fellenius, "Calculation of stability of earth dams," *Proceedings of the Second Congress on Large Dams*, vol. 4, pp. 445–463, 1936.

[3] A. W. Bishop, "The use of the slip circle in the stability analysis of slopes," *Géotechnique*, vol. 5, no. 1, pp. 7–17, 1955.

[4] N. R. Morgenstern and V. E. Price, "The analysis of stability of general slip surfaces," *Géotechnique*, vol. 15, no. 1, pp. 79–93, 1965.

[5] E. Spencer, "A method of analysis of the stability of embankments assuming parallel inter-slice forces," *Géotechotechnique*, vol. 17, no. 1, pp. 11–26, 1967.
[6] S. K. Sarma, "Stability analysis of embankments and slopes," *Journal of the Geotechnical Engineering Division*, vol. 105, no. 12, pp. 1511–1524, 1979.
[7] W. F. Chen, M. W. Giger, and H. Y. Fang, "On the limit analysis of stability of slopes," *Soils and Foundations*, vol. 9, no. 4, pp. 23–32, 1969.
[8] W.-F. Chen, *Limit Analysis and Soil Plasticity*, Elsevier, Amsterdam, the Netherlands, 1975.
[9] K. Karal, "Application of energy method," *Journal of the Geotechnical Engineering Division*, vol. 103, no. 5, pp. 381–397, 1977.
[10] K. Karal, "Energy method for soil stability analyses," *Journal of the Geotechnical Engineering Division*, vol. 103, no. 5, pp. 431–445, 1977.
[11] R. L. Michalowski, "Slope stability analysis: a kinematical approach," *Géotechnique*, vol. 45, no. 2, pp. 283–293, 1995.
[12] R. L. Michalowski, "Stability charts for uniform slopes," *Journal of Geotechnical and Geoenvironmental Engineering*, vol. 128, no. 4, pp. 351–355, 2002.
[13] J. Kumar, "Slope stability calculations using limit analysis," in *Slope Stability 2000*, pp. 239–249, ASCE Special Publication, 2000.
[14] J. Kumar, "Stability factors for slopes with nonassociated flow rule using energy consideration," *International Journal of Geomechanics*, vol. 4, no. 4, 2004.
[15] I. B. Donald and Z. Chen, "Slope stability analysis by the upper bound approach: fundamentals and methods," *Canadian Geotechnical Journal*, vol. 34, no. 6, 1997.
[16] Z. Chen, J. Wang, Y. Wang, J.-H. Yin, and C. Haberfield, "A three-dimensional slope stability analysis method using the upper bound theorem Part II: numerical approaches, applications and extensions," *International Journal of Rock Mechanics and Mining Sciences*, vol. 38, no. 3, pp. 379–397, 2001.
[17] Z. Chen, "Limit analysis for the classic problems of soil mechanics," *Chinese Journal of Geotechnical Engineering*, vol. 24, no. 1, pp. 1–11, 2002.
[18] T. K. Nian, G. Q. Chen, M. T. Luan, Q. Yang, and D. F. Zheng, "Limit analysis of the stability of slopes reinforced with piles against landslide in nonhomogeneous and anisotropic soils," *Canadian Geotechnical Journal*, vol. 45, no. 8, pp. 1092–1103, 2008.
[19] R. L. Michalowski and A. Drescher, "Three-dimensional stability of slopes and excavations," *Géotechnique*, vol. 59, no. 10, pp. 839–850, 2009.
[20] J. Kumar and P. Samui, "Stability determination for layered soil slopes using the upper bound limit analysis," *Geotechnical & Geological Engineering*, vol. 24, pp. 1803–1819, 2006.
[21] Z. Sun, J. Li, Q. Pan, D. Dias, S. Li, and C. Hou, "Discrete kinematic mechanism for nonhomogeneous slopes and its application," *International Journal of Geomechanics*, vol. 18, no. 12, 2018.
[22] L. Wang, D.'an Sun, and L. Li, "Three-dimensional stability of compound slope using limit analysis method," *Canadian Geotechnical Journal*, vol. 56, no. 1, pp. 116–125, 2019.
[23] M. Chwała, "Upper-bound approach based on failure mechanisms in slope stability analysis of spatially variable *c-φ* soils," *Computers and Geotechnics*, vol. 135, Article ID 104170, 2021.
[24] A. V. Lyamin and S. W. Sloan, "Lower bound limit analysis using non-linear programming," *International Journal for Numerical Methods in Engineering*, vol. 55, no. 5, pp. 573–611, 2002.
[25] A. V. Lyamin and S. W. Sloan, "Upper bound limit analysis using linear finite elements and non-linear programming," *International Journal for Numerical and Analytical Methods in Geomechanics*, vol. 26, no. 2, pp. 181–216, 2002.
[26] K. Krabbenhoft, A. V. Lyamin, M. Hjiaj, and S. W. Sloan, "A new discontinuous upper bound limit analysis formulation," *International Journal for Numerical Methods in Engineering*, vol. 63, no. 7, pp. 1069–1088, 2005.
[27] A. Makrodimopoulos and C. M. Martin, "Upper bound limit analysis using simplex strain elements and second-order cone programming," *International Journal for Numerical and Analytical Methods in Geomechanics*, vol. 31, no. 6, pp. 835–865, 2007.
[28] D.-P. Deng, L. Li, and L.-H. Zhao, "Stability analysis of a layered slope with failure mechanism of a composite slip surface," *International Journal of Geomechanics*, vol. 19, no. 6, 2019.
[29] W. Zhao, L. Zhao, and D. Deng, "Improved sliding surface search method for stability analysis of complex slopes," *Procedia Earth and Planetary Science*, vol. 5, pp. 88–93, 2012.
[30] J.-C. Jiang and T. Yamagami, "Charts for estimating strength parameters from slips in homogeneous slopes," *Computers and Geotechnics*, vol. 33, no. 6-7, pp. 294–304, 2006.
[31] J. L. Wang and Y. R. Zheng, et al."Discussion on upper-bound method of limit analysis for geotechenical material," *Rock and Soil Mechanics*, vol. 24, no. 4, pp. 538–544, 2003.
[32] A. R. Zolfaghari, A. C. Heath, and P. F. McCombie, "Simple genetic algorithm search for critical non-circular failure surface in slope stability analysis," *Computers and Geotechnics*, vol. 32, pp. 139–152, 2005.
[33] Y. M. Cheng, L. Li, and S. C. Chi, "Performance studies on six heuristic global optimization methods in the location of critical slip surface," *Computers and Geotechnics*, vol. 34, no. 6, pp. 462–484, 2007.